Convergency of the iterative process and numerical error in acoustical analysis with the fast multipole boundary element method

Tetsuya Sakuma (1, 2), Yosuke Yasuda (2)

(1) Institut für Technische Akustik, RWTH Aachen, Templergraben 55, 52056 Aachen

(2) Institute of Environmental Studies, The University of Tokyo, 7-3-1 Hongo, Bunkyo-ku, Tokyo 113-0033 Japan

1. Introduction

The fast multipole boundary element method (FMBEM) [1], applying the fast multipole algorithm (FMA) [2] to BE analysis with the iterative solution, has a possibility of drastic acceleration and memory saving for large-scale 3D acoustical problems. Although we have already developed the concrete setup for two sets of formulations, that is, the regular and the hypersingular boundary integral equations, the following aspects have not yet been clarified with relation to the types of formulation and the nature of problems: (i) convergency of the iterative process, (ii) numerical error, regarding the uniqueness problem. In this report, we settle exterior and interior problems with changing the acoustical impedance of the surface, and execute numerical calculation in three ways of FMBEM based on the regular, hypersingular and combined formulations, and also with the conventional BEM.

2. Numerical method

2.1. Outline of FMBEM

The FMBEM achieves matrix-vector multiplications in iterative solution for BEM by evaluating interactions between cells clustering boundary elements, where potentials of elements are accumulated as multipole coefficients at the cell's centroid. As an efficient strategy, a hierarchical structure for cells is adopted, where a cubic cell circumscribing the whole boundary is determined as the root cell, and it is divided into child cells at the lower level in turn. The accumulation of potentials is executed through the following transformation of Green's function (Figure 1):

$$G(\mathbf{r}_\mathrm{p},\mathbf{r}_\mathrm{q}) = \frac{jk}{16\pi^2}\oint E^{\mathrm{C}_L}_{\mathrm{p}}\left(\prod_{l=1}^{L-1} E^{\mathrm{C}_l}_{\mathrm{C}_{l+1}}\right) T^{\mathrm{G}_I}_{\mathrm{C}_I}\left(\prod_{l=1}^{L-1} E^{\mathrm{G}_{l+1}}_{\mathrm{G}_l}\right) E^{\mathrm{q}}_{\mathrm{G}_L}\, d\hat{\mathbf{k}}, \qquad (1)$$

where $E^{\mathrm{Y}}_{\mathrm{X}} = \exp\left(j\mathbf{k}\cdot\mathbf{r}_{\mathrm{XY}}\right)$, $T^{\mathrm{Y}}_{\mathrm{X}} = \sum_{l=0}^{N^I_\mathrm{c}} j^l(2l+1)h^{(1)}_l(kr_{\mathrm{XY}})P_l(\hat{\mathbf{k}}\cdot\hat{\mathbf{r}}_{\mathrm{XY}})$, $\mathbf{k}$ is the wave number vector, $\hat{\mathbf{k}} = \mathbf{k}/k$, $\oint d\hat{\mathbf{k}}$ represents the spherical integral, L is the number of the lowest level, and I is the number of the level to evaluate interaction between cells. Interactions between non-adjacent cells are numerically evaluated at each level, instead of those between elements. For full details of the algorithm, refer to [1].

2.2. Three kinds of formulations

Applying the FMBEM to the regular and the hypersingular formulations with constant elements gives the following equations:

$$(\mathbf{E}+\mathbf{B}+\mathbf{C})\cdot\mathbf{p} = j\omega\rho\mathbf{A}\cdot\mathbf{v}, \quad (2) \qquad (\mathbf{G}+\mathbf{H}+\mathbf{J})\cdot\mathbf{p} = j\omega\rho(\mathbf{F}+\mathbf{I})\cdot\mathbf{v}, \quad (3)$$

where $E_{ij} = -\frac{1}{2}\delta_{ij}$, $I_{ij} = \frac{1}{2}\delta_{ij}\Big|_{\Gamma_1}$, $J_{ij} = \frac{jk}{2z_j}\delta_{ij}\Big|_{\Gamma_2}$,

$$\begin{bmatrix} A_{ij} \\ B_{ij} \\ C_{ij} \end{bmatrix} = \frac{jk}{16\pi^2}\oint E^{\mathrm{C}_L}_{i}\left(\prod_{l=1}^{L-1} E^{\mathrm{C}_l}_{\mathrm{C}_{l+1}}\right) T^{\mathrm{G}_I}_{\mathrm{C}_I}\left(\prod_{l=1}^{L-1} E^{\mathrm{G}_{l+1}}_{\mathrm{G}_l}\right) \begin{bmatrix} \alpha_j \\ \beta_j \\ \gamma_j \end{bmatrix} d\hat{\mathbf{k}}, \qquad (4)$$

$$\begin{bmatrix} F_{ij} \\ G_{ij} \\ H_{ij} \end{bmatrix} = \frac{-k^2}{16\pi^2}\oint (\mathbf{n}_i\cdot\hat{\mathbf{k}}) E^{\mathrm{C}_L}_{i}\left(\prod_{l=1}^{L-1} E^{\mathrm{C}_l}_{\mathrm{C}_{l+1}}\right) T^{\mathrm{G}_I}_{\mathrm{C}_I}\left(\prod_{l=1}^{L-1} E^{\mathrm{G}_{l+1}}_{\mathrm{G}_l}\right) \begin{bmatrix} \alpha_j \\ \beta_j \\ \gamma_j \end{bmatrix} d\hat{\mathbf{k}}, \qquad (5)$$

$$\alpha_j = \int_{\mathrm{e}_j\in\Gamma_1} E^{\mathrm{q}}_{\mathrm{G}_L} dS_\mathrm{q},\ \beta_j = jk\int_{\mathrm{e}_j} E^{\mathrm{q}}_{\mathrm{G}_L}(\mathbf{n}_\mathrm{q}\cdot\hat{\mathbf{k}})dS_\mathrm{q},\ \gamma_j = \frac{jk}{z_j}\int_{\mathrm{e}_j\in\Gamma_2} E^{\mathrm{q}}_{\mathrm{G}_L} dS_\mathrm{q},$$

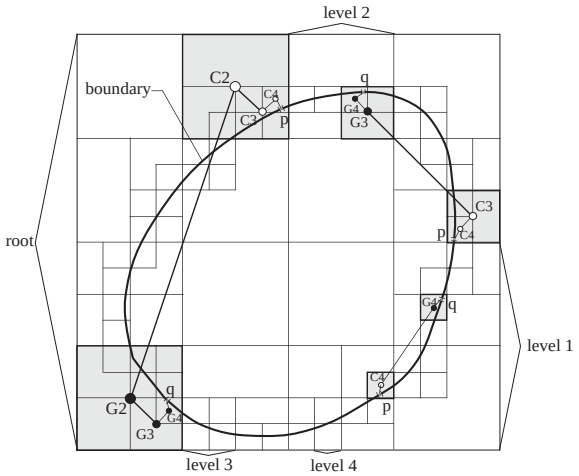

Figure 1. 2D diagram of hierarchical cell structure (L = 4), with illustrating three pathes for evaluating influence from point q to point p (I = 2, 3, 4).

e_j is the j-th element, Γ_1/Γ_2 are vibration/absorption boundaries. According to Burton-Miller's formulation [3] with the combined factor $\alpha = 1/jk$ [4], the following expression is also obtained:

$$((\mathbf{E}+\mathbf{B}+\mathbf{C}) + \alpha(\mathbf{G}+\mathbf{H}+\mathbf{J}))\cdot\mathbf{p} = j\omega\rho(\mathbf{A}+\alpha(\mathbf{F}+\mathbf{I}))\cdot\mathbf{v}, \qquad (6)$$

where

$$\begin{bmatrix} A_{ij}+\alpha F_{ij} \\ B_{ij}+\alpha G_{ij} \\ C_{ij}+\alpha H_{ij} \end{bmatrix} = \frac{jk}{16\pi^2}\oint (1+\mathbf{n}_i\cdot\hat{\mathbf{k}}) E^{\mathrm{C}_L}_{i}\left(\prod_{l=1}^{L-1} E^{\mathrm{C}_l}_{\mathrm{C}_{l+1}}\right) T^{\mathrm{G}_I}_{\mathrm{C}_I}\left(\prod_{l=1}^{L-1} E^{\mathrm{G}_{l+1}}_{\mathrm{G}_l}\right) \begin{bmatrix} \alpha_j \\ \beta_j \\ \gamma_j \end{bmatrix} d\hat{\mathbf{k}}. \qquad (7)$$

The difference among equations (4), (5) and (7) can be seen only in the left-end term in the integral, therefore a large part of the computational procedures are common to three formulations. Thus the FMBEM requires almost the same amount of computational load in the three ways.

3. Models and Conditions

A surface of a cube with sides d m is considered for exterior and interior problems. Boundary conditions on the surface are as follows:

Exterior problem: All boundaries are given vibration velocities to be equal to particle velocities in the free field with a point source at the cube's center. Naturally, this exterior field is equivalent to the imaginary free field with the point source, which enables comparison between numerical and theoretical results.

Interior problem: A point source is located at the cube's center. All boundaries are given uniform absorption coefficents (α = 0, 0.5, 1).

The surface is divided into 3750 rectangular elements, with 25 divisions per side. In FMBEM application, the Bi-CGSTAB is used for the iterative process, and a cell hierarchy of L = 3 is used.

4. Results and Discussions

4.1. Exterior problem

Figure 2 shows the errors in the sound pressure at the center on the square face, calculated with BEM and FMBEM through the three kinds of formations. Similar tendencies can be seen in the errors with BEM

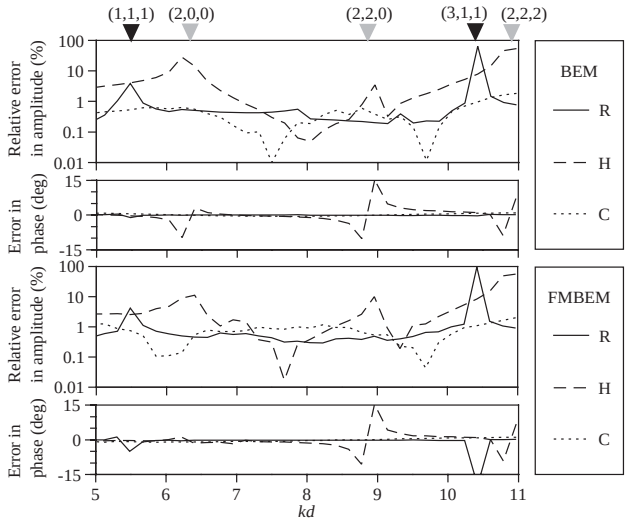

Figure 2. Errors in the sound pressure calculated with BEM and FMBEM in the form regular (R), hypersingular (H), and combined (C).

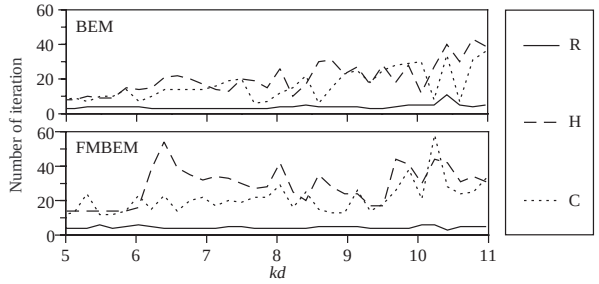

Figure 3. Numbers of iteration in the calculations with BEM and FMBEM in the form regular (R), hypersingular (H), and combined (C).

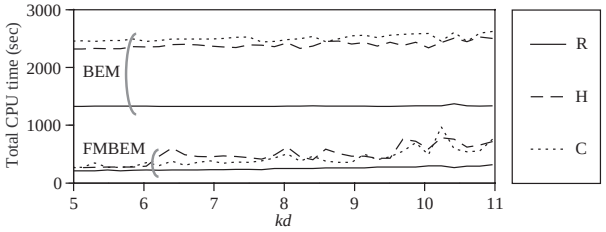

Figure 4. Total processing time with BEM and FMBEM in the form regular (R), hypersingular (H), and combined (C).

and FMBEM, where the accuracy spoils at the fictitious eigenfrequencies except in the combined form. Figure 3 shows the numbers of iteration required for solving liner systems. No clear relation is seen between the number of iteration and the fictitious eigenfrequencies. Remarkably, the regular form requires smaller numbers, suggesting that the hypersingular form causes slow convergence. Figure 4 shows the total processing time. Contrary to the case with BEM, the CPU time with FMBEM strongly depends on the number of iteration. Generally, the advantage of FMBEM over BEM is clearly seen in CPU time, and in addition, FMBEM used about 1/4 amount of memory for BEM.

4.2. Interior problem

Figure 5 shows the differences in the sound pressure level at the center on the square face, calculated with BEM and FMBEM in the regular and the hypersingular forms under the three boundary conditions. Under the rigid boundary condition, the maximum difference of 3 dB is seen when using the hypersingular form, and those between BEM and FMBEM in the regular form are very little. Figure 6 shows the numbers of iteration.

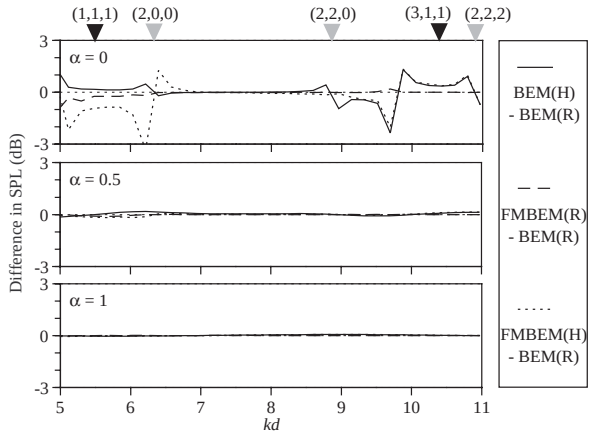

Figure 5. Differences in the SPL calculated with BEM and FMBEM in the form regular (R) and hypersingular (H), referring to the results with BEM(R), under the three boundary conditions.

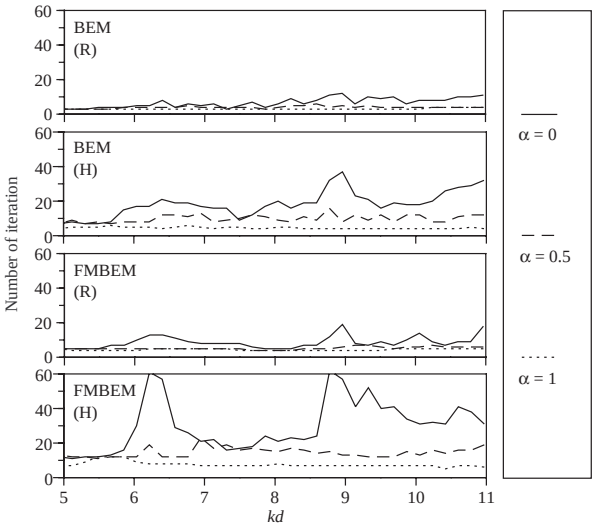

Figure 6. Numbers of iteration in the calculations with BEM and FMBEM in the form regular (R) and hypersingular (H), under the three boundary conditions.

Basically, weak damping in the cavity tends to raise the iteration number around the eigenfrequencies, however, not remarkably if using the regular form which is natural to treat interior problems. Regarding the processing time and the memory requirements, the general tendency in the internal problem is almost the same as in the external problem.

5. Conclusions

For external problems, the FMBEM in the combined form is valid to overcome the fictitious eigenfrequency difficulties, however, which requires more processing time than in the regular form. For interior problems, the FMBEM in the regular form has almost the same accuracy as the BEM has, and the iteration number does not strongly depend on the damping in the space. In both problems, whether BEM or FMBEM, the hypersingular form causes slow convergence in the iterative solution.

References

[1] T. Sakuma: Fast multipole boundary element method for predicting sound fields. Proc. Inter-Noise 99 (1999) 1639-1644.

[2] L. Greengard, V. Rokhlin: A fast algorithm for particle simulations. J. Comput. Phys. 73 (1987) 325-348.

[3] A. J. Burton, G. F. Miller: The application of integral equation methods to the numerical solution of some exterior boundary value problems. Proc. R. Soc. London, Ser. A 323 (1971) 201-210.

[4] K. A. Cuneface, G. Koopmann: A boundary element method for acoustic radiation valid for all wavenumbers. J. Acoust. Soc. Am. 85 (1989) 39-48.